SPACEBORNE GNSS-REFLECTOMETRY FOR SHIP-DETECTION APPLICATIONS: IMPACT OF ACQUISITION GEOMETRY AND POLARIZATION

Alessio Di Simone[1,2], Leonardo M. Millefiori[1], Gerardo Di Martino[2], Antonio Iodice[2], Daniele Riccio[2], Giuseppe Ruello[2], Paolo Braca[1], Peter Willett[3]

[1] NATO Science and Technology Organization Centre for Maritime Research and Experimentation (STO CMRE), 19126, La Spezia, Italy

[2] Department of Information Technology and Electrical Engineering, University of Naples Federico II, 80125, Naples, Italy

[3] Department of Electrical and Computer Engineering, University of Connecticut, Storrs, CT 06269 USA

ABSTRACT

In this paper, a comparative study of spaceborne Global Navigation Satellite System (GNSS)-Reflectometry for ship detection applications is provided. The analysis is conducted by evaluating the impact of 1) the acquisition geometry and 2) the received signal polarization on ship detectability in GNSS-R data. In particular, the backscattering acquisition geometry is demonstrated to be more suitable for ship detection applications, thus allowing for the detection of 20 m-length ships. Even very large ships are hardly detectable in the conventional forward-scattering geometry. Moreover, receiving right-hand circular polarization is demonstrated to provide significant improvements of the signal-to-noise-plus-clutter with respect to the conventional left-hand circular polarization channel, conventionally exploited in GNSS-R remote sensing. The study is based on a numerical tool for the bistatic radar cross section of the ship, which is presented in a companion paper.

Index Terms— maritime surveillance; ship detection; GNSS-Reflectometry; bistatic radar; backscattering geometry

1. INTRODUCTION

Conventional Global Navigation Satellite System (GNSS)-Reflectometry works in the forward-scattering geometry of acquisition, where most of the received signal comes from the specular reflection point and a surrounding region, called glistening zone. This signal is processed to deliver informative GNSS-R observables, such as the delay waveform and the 2-D delay-Doppler Map (DDM). Such data are currently exploited in ocean remote sensing to infer geophysical parameters of the sea surface, such as wind speed, sea surface height and sea state [1-3]. Very recently, the GNSS-R technology has been used for ship detection applications [4-8]. In [4], an automatic algorithm for the detection of sea targets using GNSS-R delay-Doppler Map (DDM) is presented. The detector is based on a sea clutter suppression step, which enables the detection of large targets even from spaceborne GNSS-R platforms. However, the conventional forward-scattering geometry opens numerous issues in the detectability of ship targets as already illustrated in [5], [9]. Indeed, benefits of the backscattering geometry were already shown in [5], where a simplified radar cross section (RCS) model was used for describing the ship return. In particular, the ship-sea interaction geometry was modeled via a perfectly conducting corner reflector faced to the GNSS transmitter.

This paper provides a comparative analysis of the conventional forward-scattering geometry and the backscattering one, where the transmitter, receiver and target are aligned. The study is based on a numerical tool for the evaluation of the bistatic RCS of the ship, which is presented in a companion paper [10]. Another relevant aspect analyzed in this paper concerns the effects of the received signal polarization on ship detectability. Conventional GNSS-R measures the left-hand circular polarization (LHCP) of the signal reflected off the sea surface, since this is much higher than the opposite right-hand circular polarization (RHCP), which is the polarization adopted by the GNSS transmitter [11].

This paper is organized as follows. The experimental setup used to assess ship detectability in different acquisition geometries and systems is described in section 2. In section 3, the conventional forward-scattering configuration is compared with the backscattering one to show the main limits of the former and the benefits of the latter for ship detection purposes. Then, the effects of the received signal polarization on ship detectability is assessed by comparing the RL cross-polarization channel commonly exploited in GNSS-R receivers with the RR co-polarization one. Main conclusions are drawn in section 4.

2. EXPERIMENTAL SETUP

In order to assess ship detectability in GNSS-R data, we evaluate the signal-to-noise-plus-clutter-ratio (SNCR), defined as:

$$SNCR = \frac{P_{r,ship}}{P_n + P_{r,sea}} \quad (1)$$

where

$$P_{r,ship} = P_t G_t G_r \frac{1}{(4\pi)^3}\left(\frac{\lambda \cos\vartheta \cos\vartheta_s}{h_t h_r}\right)^2 \sigma_{ship} \quad (2)$$

$$P_{r,sea} = P_t G_t G_r \frac{1}{(4\pi)^3}\left(\frac{\lambda \cos\vartheta \cos\vartheta_s}{h_t h_r}\right)^2 \sigma_{sea} \quad (3)$$

$$P_n = \frac{k_B T_E}{T_i} \quad (4)$$

are the target received power, sea surface received power (also referred to as sea clutter), and thermal noise power, respectively. The symbols used are defined in Table I, where values are reported for GPS as the transmitting GNSS and TDS-1 as the GNSS-R receiver. The incoherent integration time T_i accounts for the multi-look processing typically performed onboard GNSS-R receivers.

TABLE I
LIST OF SYMBOLS. VALUES ARE REPORTED IN SI UNITS FOR GPS AND TDS-1

Symbol	Parameter	Value
$P_{r,ship}$	Received power from ship	Variable
$P_{r,sea}$	Received power from sea surface	Variable
P_n	Noise power at the receiver	3.12×10^{-18}
P_t	Transmitted power	26.61
G_t	Transmitter antenna gain	19.95
G_r	Receiver antenna gain	25.12
λ	Signal wavelength	0.19
h_t	Transmitter altitude	2.02×10^{7}
h_r	Receiver altitude	5.40×10^{5}
σ_{ship}	Radar cross section of the ship	Variable
σ_{sea}	Radar cross section of sea surface	Variable
k_B	Boltzmann constant	1.38×10^{-23}
T_E	Noise temperature of the receiver	225.70
T_i	Incoherent integration time	1

Radar cross section of sea surface has been evaluated according to [12], while the algorithm used to compute the radar cross section of the ship is presented in the companion paper [10], where the multiple bounce contributions between the ship hull and the sea surface are accounted for. According to [10], the radar cross section of both the ship and sea surface depend on the relative position between transmitter, receiver and target, and the sea state via the RMS slope α. In addition, the radar signal scattered from the ship also depends on the target aspect angle, describing the ship orientation with respect to the transmitting station. The equations linking the RMS slope to the sea state and wind speed v are reported in [13] and shown here for clarity purposes:

$$\alpha(SS) = 0.055 + 0.007SS, SS = 0,1,\ldots 8 \text{ (rad)} \quad (5)$$

$$v(SS) = 1 + 2SS + \left(\frac{SS}{5.3}\right)^6 \text{ (m/s)} \quad (6)$$

where SS stands for the Douglas sea state number (SS = 0,1,…,8).

3. NUMERICAL RESULTS

In this section, numerical results of the comparative analysis are shown. The SNCR is evaluated according to (1)-(4) and assuming the parameter values reported in Table I. The ship target is assumed to be 300×60×10 m^3, unless otherwise stated. It is worth mentioning that the proposed numerical analysis has been conducted assuming a resolution cell size 10×10 km^2, which is reasonable in spaceborne GNSS-R for delay-Doppler cells close to the specular reflection point. However, in the backscattering geometry, smaller resolution cell size may be considered [14].

3.1. The impact of the acquisition geometry

In order to evaluate the role of the GNSS-R acquisition geometry on ship detectability, the conventional forward-scattering configuration is compared with the backscattering one. Results are presented in Fig. 1, where the SNCR is shown as a function of the ship aspect angle for different sea states and assuming the GNSS look angle ϑ = 10° (Fig. 1a) and ϑ = 20° (Fig. 1b). The presence of multiple-bounce reflections between the sea surface and the ship hull makes the signal scattered from the ship stronger in the backscattering direction rather than in the forward one, where sea clutter dominates the received signal. This is true for any ship orientation and sea state. However, these parameters greatly influence the ship SNCR. Thus, in the backscattering configuration, the SNCR is highest for aspect angles close to 0° and 90°, i.e., when a ship side is facing the transmitter. In such configurations, calm sea is demonstrated

to be the most favorable sea state to ship detection applications. Moreover, the lowest SNCR is achieved for aspect angles close to 45°; very high sea makes the received signal less sensitive to the target aspect angle, and, then, is expected to ensure detection performance more robust against ship orientation. Finally, the highest SNCR values are achieved with GNSS look angle $\vartheta = 20°$.

3.2. The impact of the receiving polarization channel

The analysis of the impact of the receiving polarization channel in the detectability of ship targets is presented in Fig. 2, where the SNCR is shown as a function of the ship aspect angle for different sea states and assuming LHCP and RHCP as receiving channels. The GNSS look angle is $\vartheta = 15°$ (Fig. 2a) and $\vartheta = 30°$ (Fig. 2b). For ship detection applications, the RHCP channel is demonstrated to be more suitable than the LHCP, typically exploited in GNSS-R remote sensing over the ocean. This result is justified by the lower sea clutter in the co-pol circular channel and the stronger ship echo due to the multiple reflections. The highest gain is experienced for very calm sea, where an increase of more than 40 dB is achieved moving from LHCP to RHCP (see Fig. 2a). However, a polarization gain larger than 20 dB is obtained with very high sea.

3.3. Observable ship targets in GNSS-R data

Results obtained in the previous analysis are exploited here to investigate the ship targets size observable in GNSS-R data. In particular, this analysis quantifies the minimum ship length necessary to achieve a positive SNCR in dB. Results are shown in Fig. 3 as a function of the ship orientation and for different sea states. The GNSS look angle is $\vartheta = 15°$ (Fig. 3a) and $\vartheta = 30°$ (Fig. 3b). Again, the implemented GNSS-R satellite simulates the U.K. TDS-1 receiver, apart for the backscattering acquisition geometry and the receiving RHCP channel. It is demonstrated that 20 m-ship targets ensure a positive SNCR in dB in certain conditions, namely, very calm sea and aspect angles close to either 0° or 90°. On the other hand, no reasonable targets are expected to be detectable for aspect angles close to 45°.

4. CONCLUSIONS

In this paper, a comparative analysis has been conducted to assess the feasibility of the ship detection problem in spaceborne GNSS-R data. The conventional GNSS-R technology has been analyzed in two respects, namely the acquisition geometry and the receiving polarization channel. Concerning the first point, the forward-scattering geometry, typically adopted in GNSS-R missions, has been compared with the backscattering one. Numerical results showed that better detection performance is expected in the latter configuration, due to the much lower sea clutter in the backscattering direction. In addition, the conventional LHCP channel has been demonstrated to be less suitable for the ship detection problem with respect to the co-pol RHCP channel, typically exploited in GNSS-R remote sensing. In particular, RHCP provided a polarization gain of more than 40 dB in very calm sea condition. In such a configuration, ships up to 20 m are demonstrated to be detectable. However, a proper system design may be required to filter out the direct path when using the RHCP polarization channel.

5. ACKNOWLEDGMENTS

This research has been funded by the Office of Naval Research under contract N00014-16-13157, and this support is acknowledged with thanks to John Tague and Michael Vaccaro. There is parallel support to ONR-Global.

6. REFERENCES

[1] J. Marchan-Hernandez, E. Valencia, N. Rodriguez-Alvarez, I. Ramos-Perez, X. Bosch-Lluis, A. Camps, F. Eugenio, and J. Marcello, “Sea-State Determination using GNSS-R Data,” *IEEE Geoscience and Remote Sensing Letters*, vol. 7, no. 4, pp. 621–625, 2010.

[2] M. P. Clarizia, C. Ruf, P. Jales, and C. Gommenginger, “Spaceborne GNSS-R Minimum Variance Wind Speed Estimator,” *IEEE Trans. Geosci. Remote Sens.*, vol. 52, no. 11, pp. 6829-6843, 2014.

[3] A. Rius, E. Cardellach, and M. Martín-Neira, “Altimetric Analysis of the Sea-Surface GPS-Reflected Signals,” *IEEE Trans. Geosci. Remote Sens.,* vol. 48, no. 4, pp. 2119-2127, 2010.

[4] A. Di Simone, H. Park, D. Riccio, and A. Camps, “Sea Target Detection Using Spaceborne GNSS-R Delay-Doppler Maps: Theory and Experimental Proof of Concept Using TDS-1 Data,” *IEEE J. Sel. Topics Appl. Earth Observ. Remote Sens.,* vol. 10, no. 9, pp. 4237 - 4255, Sept. 2017.

[5] M. P. Clarizia, P. Braca, C. S. Ruf, and P. Willett, "Target Detection using GPS Signals of Opportunity," in *18th International Conference on Information Fusion (Fusion)*, Washington, DC, 2015.

[6] G. Carrie, T. Deloues, J. Mametsa and S. Angelliaume, "Ship Detection Based on GNSS Reflected Signals: An Experimental Plan," in *Proc. Space Reflecto,* Calais, France, 2011.

[7] Y. Lu, D. Yang, W. Li, J. Ding, and Z. Li, "Study on the New Methods of Ship Object Detection Based on GNSS Reflection," *Marine Geodesy*, vol. 32, no. 1, pp. 22-30, 2013.

[8] A. Di Simone, A. Iodice, D. Riccio, A. Camps, and H. Park, "GNSS-R: A Useful Tool for Sea Target Detection in Near Real-Time," *2017 IEEE 3rd International Forum on Research and Technologies for Society and Industry (RTSI),* Modena, 2017, pp. 1-6.

[9] S. L. Ullo, G. Giangregorio, M. di Bisceglie, C. Galdi, M. P. Clarizia and P. Addabbo, "Analysis of GPS Signals Backscattered from a Target on the Sea Surface," *2017 IEEE International Geoscience and Remote Sensing Symposium (IGARSS)*, Fort Worth, TX, 2017, pp. 2062-2065.

[10] W. Fuscaldo, A. Di Simone, L. M. Millefiori, D. Riccio, G. Ruello, P. Braca, and P. Willett, “Electromagnetic Modeling of Ships in Maritime

Scenarios: Geometrical Optics Approximation," *2018 IEEE International Geoscience and Remote Sensing Symposium (IGARSS)*, (submitted).

[11] V. U. Zavorotny and A. G. Voronovich, "Scattering of GPS Signals from the Ocean with Wind Remote Sensing Application," *IEEE Trans. Geosci. Remote Sens.*, vol. 38, no. 2, pp. 951-964, Mar 2000.

[12] G. Franceschetti, A. Iodice, and D. Riccio, "A Canonical Problem in Electromagnetic Backscattering from Buildings," *IEEE Trans. Geosci. Remote Sens.,* vol. 40, no. 8, pp. 1787–1801, 2002.

[13] D. K. Barton, "*Radar Equations for Modern Radar*," 1st Edition, Artech House, cap. 9, pp. 324, 2012.

[14] M. Di Bisceglie, G. Di Martino, A. Di Simone, C. Galdi, A. Iodice, D. Riccio, G. Ruello, "Two-Scale Model for the Evaluation of Sea-Surface Scattering in GNSS-R Ship Detection Applications," *2018 IEEE International Geoscience and Remote Sensing Symposium (IGARSS)*, (submitted).

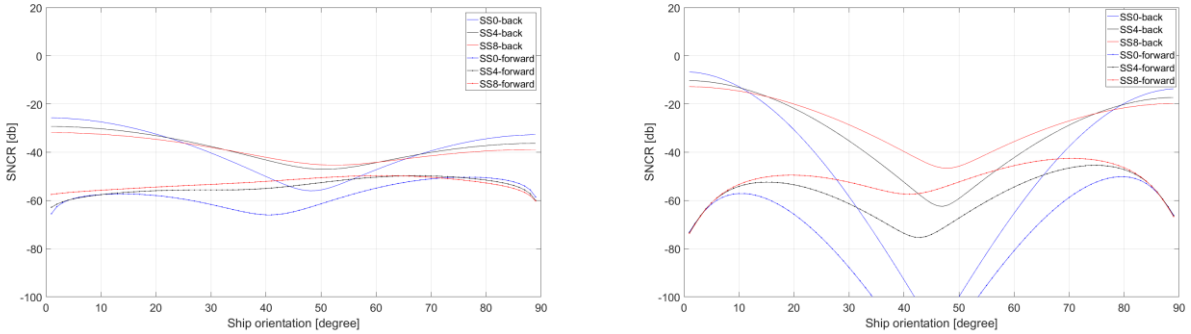

Fig. 1: SNCR of the ship target as a function of the ship aspect angle for SS0 (calm sea, blue lines), SS4 (moderate sea, black lines), SS8 (very high sea, red lines) in the backscattering (solid lines) and forward scattering (dashed lines) geometric configurations. Receiving polarization channel is LHCP. (a) $\vartheta = 10°$, (b) $\vartheta = 20°$.

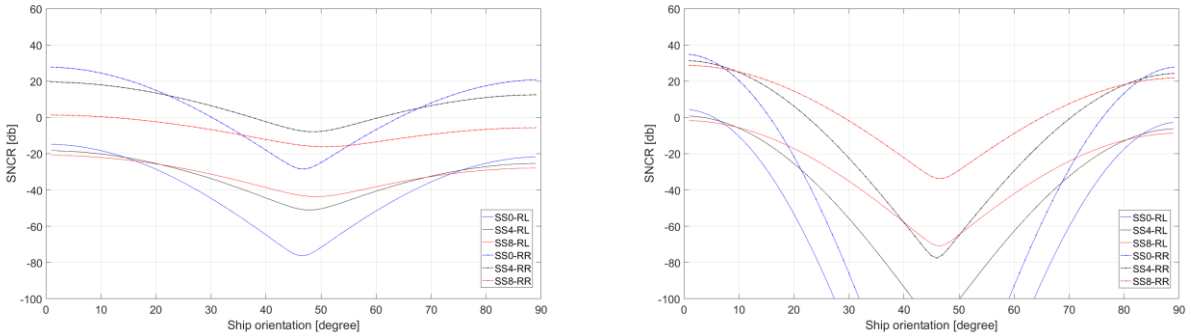

Fig. 2: SNCR of the ship target as a function of the ship aspect angle for SS0 (calm sea, blue lines), SS4 (moderate sea, black lines), SS8 (very high sea, red lines) in the backscattering geometry assuming LHCP (solid lines) and RHCP (dashed lines) as the receiving polarization channel. (a) $\vartheta = 15°$, (b) $\vartheta = 30°$.

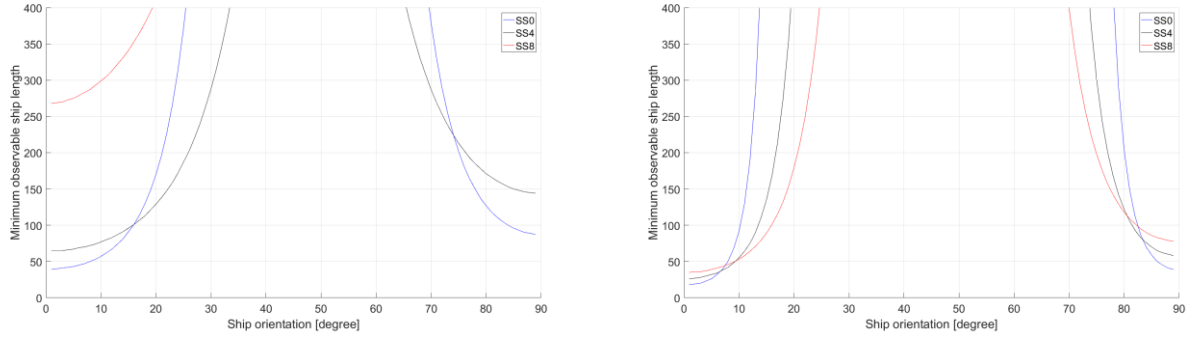

Fig. 3: Minimum ship length achieving a positive SNCR in dB in backscattering as a function of the ship orientation and for different sea states. Receiving polarization channel is RHCP. (a) $\vartheta = 15°$, (b) $\vartheta = 30°$.